

Predicting CT Images with Attenuation Correction Factor for Using Neighbourhood Approach

Srinivas Babu Gottipati¹, Gowri Thumber²

Submitted: 22/07/2022

Accepted: 25/09/2022

Abstract: Magnetic Resonance Imaging (MRI) and Computed Tomography (CT) imaging were incorporated and correlated with each other. These two clinical were adjusted with the attenuation factor between them. As both the clinical imaging techniques use the same hardware leads to time consumption with a low rate of prediction in the existing systems. Therefore, in this paper, predicting CT (p-CT) images by accessing MRI data was implemented with nearest neighbor cluster method identification. The proposed model reduces the training cost and enhances the prediction rate by minimizing the time of execution. PET/MRI helps in understanding the regions of soft tissue and functional tissues, which includes the internal body parts. These datasets out to investigate scientific prerequisites that would perchance be acquired from brain PET/MRI imaging mainly primarily based absolutely on caseload. In this paper, the performance metrics compared are Peak Signal Noise Ratio (PSNR), Mean Absolute Error (MAE). The performance of PET/MRI to quit the imaging modality wish to investigate neurologic and oncologic stipulations related to handy tissues is highlighted. Clinical factors of PET/MRI and its software program to scientific conditions are illustrated with examples extracted from the authors' prior experience.

Keywords: PET, CT, MRI, KNN, Attenuation, PCT

1. Introduction

CT imaging uses x-ray measurements to produce axial clinical images of various body parts. It was a similar procedure for MRI, X-Ray, and Positron Emission Tomography (PET). For a clear vision of brain parts and depth levels, a contrast will be for some conditions and for other conditions might not. This leads to heavy exposure to the radiation generated while CT imaging. Mainly in the course of cancer treatment, CT imaging was conducted [1]. Notwithstanding, the utilization of CT checks is advised, as a result of radiation from the patient's body. Obviously, around 0.4% of US disease patients are analyzed utilizing past CT outputs, and this rundown ought to be pretty much as high as 1.5 to 2% in the future [2]. Moreover, a developing imaging instrument, a cutting-edge PET scanner, and MRI are trading CT use for MRI. Notwithstanding, it is trying to foresee the coefficients of harm to MR pictures since MRI examines that the person's

vocal strings are connected with proton thickness, not the electron thickness estimations expected for AC. For instance, with the utilization of style MRI arrangements, all air, and joint bone produce low signals, and markdown the coefficients are unlike altogether, as confirmed in Figure 1.

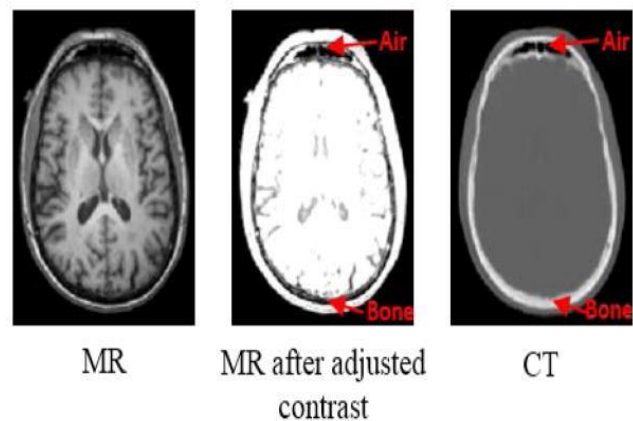


Figure 1: CT Extraction from MRI Images

An all-around paired sets of MRI and CT pixels from human mind. Both breeze and bone have exceptionally low reactions to MRI pictures, yet they are isolated by CT pictures. Along these lines, there is a significant need to anticipate a CT picture from a MR picture. Current assignments can be separated into four classes: Tissue order depends altogether on techniques. The straightforward thought is to initially parted the MR picture into independent tissue classes, and afterward give each

¹Srinivas Babu Gottipati

Department of ECE, NRI Institute of Technology, Vijayawada., India

ORCID ID : 0000-0002-4794-8697

Email id: gsrinivasbabu@yahoo.co.in

² Gowri Thumber, Department of ECE, GITAM University,

Visakhapatnam, India

Email id: gowrithumber78@gmail.com

ORCID ID : 0000-0002-2584-1397

* Corresponding Author Email: gsrinivasbabu@yahoo.co.in

class the correct thing to hold. Be that as it may, this kind of approach might bomb because of the presence of strange tissue preparing, like air and bone. Specifically, Zaidi et al. [3] proposed a randomized controlled preliminary dependent essentially upon the division of MRI into 5 tissue classes, fittingly as a constant variety in the division of workstations. Hsu et al. [4] has sabotaged the utilization of different MRI procedures, for example, oil imaging and fluid photography as per Dixon MRI arrangements. They confirmed that a solitary MRI filter was not to the point of isolating all the tissue classifications. Also, Berker et al [5] embedded the UTE/Dixon MRI grouping into AC stage tissues.

Map book-based approaches. These are the strategies for estimating the tension markdown map given by winding the map book rebate guide of this condition [6, 7], the utilization of the altered MR picture enrollment region between the map book and title. In any case, the full usefulness of existing strategies is generally founded on the recognition pace of the enlistment of the clinical pictures got to.

Learning-based approaches. MRI and CT imaging relation considered using a data set and used for the purpose of MR image-based prediction of CT images. While it may not be easy to analyze such relation in one way, in [8] it was proposed to create a retrieval of a combined Gaussian model for more than one route record, i.e., first is low contrasted and second is high contrasted TRR-weighted MR image. By Gaussian mixing model predicting CT images using 2 MRI images was made easy with less train data set in [9]. In [10] a similar method used to measure CT image on a single MR image. However, local archives have always been left out and the limited CT image was once small, for that purpose it is often used as an intermediate skill to direct subsequent enrolment work.

Integration of atlas-based focus strategies and sample. After investigating the atlases in the target image, the retrieval model (indicated by the location and depth of the image) was developed and applied to the target image. In [7] used a Gaussian reciprocal system was implemented. Although these types of methods will generate effective results, but their normal operation still requires more accuracy of the fine-grained classification models between the atlas and the cause of the MR images.

One more firmly related explanation of self-control is the assortment of pictures, which have a similar reason for consolidating a solitary picture into a specific sort, despite the fact that a similar kind of material is utilized. A large number of these examinations fall into the accompanying two classes:

Learning-based approaches. In T2 and T1-weighted pictures of various loads used to recreate or foresee CT pictures. However, this system was contrasted and the Fluid Attenuated (FLAIR) grouping individually from PD-weighted MRI, T1 and T2 arrangements [12]. This strategy involves irregular Forest Divisions to work as every day and

straightforward changes, done utilizing nearby records or having unique CT improvements. In [13], the creators utilized the utilization of convolution brain organizations to adjust PET picture constriction from MR picture. Notwithstanding, the neighborhood brain methodology experiences long haul preparing, from days to weeks, and its generally expected working as an option relies upon the gainful change of more than one boundary.

Models in view of models. The fundamental view in this segment is a couple of techniques dependent basically upon pictures. In the first place, the objective picture is on the scale addressed with the assistance of a chart book bundle pack of equivalent mode. Then, the following scanty coefficient was blended in with the relating map book packs of any unique strategy to quantify a well-known picture cut for that target title technique. Roy et al. utilize this interaction to wipe out more than one issue, that is to say, attractive field expectation sets the succession of a separated reverberation angle from memory and more regrettable, for example, anticipating FLAIR picture from T1-and MRI by changing T2 weight. In [14, 15, 16, and 17] T2 and pixels have a weight dissemination or elements from the T1-weighted MRI, while in T1-weighted MRI is normal MRI-weighted MRI. However, quite possibly the main inconveniences of these technique is that expectations are frequently automated because of the huge measure of work expected in the testing stage.

In this paper, we will rent an area with arbitrary wood to manage the trouble of assessing a CT picture from MRI information, with the accompanying contributions:

Nearby insights are all around developed to make CT expectations more persuading with chart book bended and title enlistments, instead of devastating enrollments.

The pieces of the picture are planned in another manner with the awareness of many segments to settle the mission for admittance to specific levels of adaptability in pivot of pictures, yet however they have added to minor primary changes. Also, guides are given with different goals toward contain generally open records and likewise a mix of all worldwide and friendly data, making the calculation stronger in the handling of a solitary picture of a similar sort. The paper was organized as follows in 2 proposed methodology was discussed, section 3 helps in discussion of the proposed model results acquired and section 4 concludes the paper with future directions.

2. Method

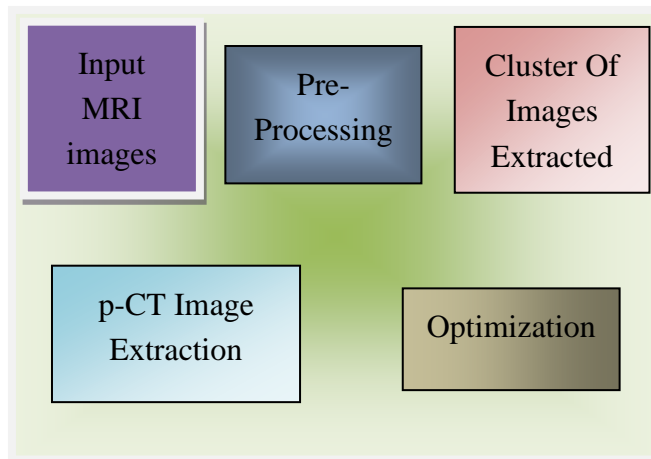


Figure 2: Block Diagram for p-CT Extraction

Figure 2 represents the block diagram for p-CT extraction, that consists of 5 stages which were explained below in details. The stages for implementation are input association, pre-processing, clustering, optimization and p-CT extraction.

2.1 INPUT MRI CT IMAGES: The publicly available MRI and CT images of similar persons were extracted from KAGGLE websites a total 53 sets combination of both MRI and CT clinical images were available.

2.2 PREPROCESSING: All the clinical images were needs to be with similar resolution and contrast points which help the data association detection to be perfect. But as motioned earlier contrast might not be used for some images this leads to non-similar texture combination between images. Therefore, a threshold model-based contrast adjustment was performed on the images considered as inputs from the datasets available. This pre-processing allows in predicting the CT images more effectively compared with intra and inter subjective tests.

2.3 CLUSTERING BASED PREDICTION: The pre-processed images were subjected to K-Nearest Neighbours (KNN) and extracted features were distributed unbalanced. The reason for considering KNN as it is one of the easiest algorithms used in Machine Learning to return up the trouble of separation in unbalanced distribution of clusters. KNN algorithms procedure facts and classify new facts factors based totally on the identical measurements (e.g., distance function). Divisions are made through a majority of votes from their neighbours.

Algorithm: Enhanced Neighbor for p-CT Recognition

INPUT: MRI-1 and MRI-2 images

Let (X_i, C_i) when $i = 1, 2, \dots, N$ be facts points. X_i ability function values & C_i capability character X_i for labels i .

If we take the variety of instructions as 'c' $C_i \in \{1, 2, 3, 4, 5, 6\}$ in all values i

X make a factor the place the label is unknown, and we would like to discover the label class the use of the algorithms of the neighbor subsequent to k .

- Calculate " $d(x, x_i)$ " $i = 1, 2, 3, 4, \dots, n$; when d suggests the Euclidean distance between two points.
- Arrange 'n' Euclidean counts listed in the following order.
- With + ve full number, take the first ok values in the sorted list.
- Find the k -points related with these distances of k .
- Let k_i capability the range of factors in the i th classification between okay factors ukuthi zero ≥ 0
- If $k_i > k_j \forall i \neq j$ put x in the type i .

OUTPUT: Learned descriptors of six image clusters

A close by neighbours is a unique case of a neighbours type subsequent to k . When the price of o_k is one ($k = 1$). In this condition, a new facts factor type will be assigned to the first neighbor.

Given the complex relationship between MRI imaging signals and hybrid PET programs remains a challenging task to generate a CT image with effective prediction rate. Due to training and testing of the models it requires to heavy datasets, time and not effective data prediction rate. In this work, an effective way to p-CT images from T1 (low contrast or with a different time) and T2 (high contrasted or the next day) MRI data with data is proposed. The proposed method uses advanced retrospective antenna (INAR) retrieval as a basic method of pre-calculating predictable matrices in order to predict inconsistent pseudo-CT patches. Strategies, including the addition of MRI / CT databases, indirect reading of MRI images, sequential search of nearby neighbours, data-driven improvements, and multi-regressor combinations, were adopted to improve efficiency.

3. Result Experiments

CT scans are crucial collection of scientific diagnoses with radiotherapy treatments. As CT pictures intensity associated with PET attenuation coefficients, they may be crucial in correcting the bargain Attenuation correction of PET pics. However, because of the excessive amount of radiation publicity on CT scans, it is recommended that the CT imaging be restrained. In addition, in the new PET and magnetic resonance imaging (MRI) scanner, entirely MR images are to be had, unluckily unrelated to the AC. These troubles drastically motivate the development of reliable CT imaging techniques from its corresponding MR photo of an associated subject.

3.1 Data Units

We tested our set of rules on two databases, as defined beneath:

To perform the tests and prove the efficiency of the proposed model a brain dataset with 20 subjects' data considered from Alzheimer's Disease Neuroimaging Initiative (ADNI), that is available on the internet publicly. Each image results with a size of 112X112X1 pixels. The set of images were collected with a time difference of 6.3 ± 9.6 sec in a day with change of 6° . This subjects for low contrasted or low resolute datasets.

With a day or less than 3 days the same similar 20 subjects' data considered from the same data set availed with similar resolution and different contrast. Even the it's like a Dice similarity coefficient. This made to use the data set for predicting CT images

We have made a one-time affirmation of the whole database. In all the checks at a sure time in this paper, if now not immediately quoted, the following stipulations have been applied:

- Packet dimension for MR image: $15 \times 15 \times 15$.
- Output pixel CT image: $3 \times 3 \times 3$.
- Number of neighboring coefficients used in K-MEANS: 6.
- Basic CT confirmation
- Data optimization.
- The closing pCT expected.
- Number of collections: 6.
- Data set size:1900.
- Minimum vary of training samples at: 500.

3.2 Quantity Estimates

To substantiate the accuracy of the prediction, we used two famous metrics: 1) we endorse whole error (MAE) and 2) most signal-to-noise (PSNR) rating:

$$MAE = \frac{\|E - \hat{E}\|}{Q}$$

$$PSNR = 10 \log \left(\frac{Q^2}{MAE} \right)$$

when E is a low-resolution CT image, \hat{E} correlated CT image, Q is the most depth of E and \hat{E} , and C is a range of vowels in the image. In general, end result of a nice bet has a limit in MAE and a large PSNR.

3.3 Comparison of Performance Metrics

We first discover our direction through a regular casual wooded area. In phase 2, we've introduced upgrades over the essential clustering set of rules and new integrated fashions. In the brand-new fashions mixed, median medians and median competence are in contrast and for that purpose are anticipated to deliver comparable outcomes. Therefore, we have selected to use the median for scanning energy because of its computer performance. However, by using combining these improvements in a regular way, we've four versions of the jungle: the primary jungle with advice version (TN-M), the wooded region with the suggest ensemble version (-SM), the usual jungle with median

abilities that includes model. (TN-MM), with a random cluster with a median of functionality ensemble version (MF-MM).

The second determine presents an accurate seen illustration of all four species. The consequences have now not modified throughout all two statistics units. We see that a deliberate location with random timber can seize continuity, coherence and smoothness in predictable outcomes, because of the fact it makes use of the residence restriction inside the area of the photograph, as cited in Section 2). This is derived from the variations between TN-M and MF-MM, and similarly among TN-MM and MF-MM. Besides, the fashion outcomes of the specific aggregate can certainly be regarded in terms of the difference among the outcomes from TN-M and TN-MM, and in addition among the results from MF-M and MF-MM. The median capability model continually presents cleaner and plenty much less noise effects in assessment to the preferred endorsed model, indicating that the latter is at danger of manufacturing an uncommon effect that is no longer currently contemporary within the outcomes of skilled trees, as cited in. Section 2).

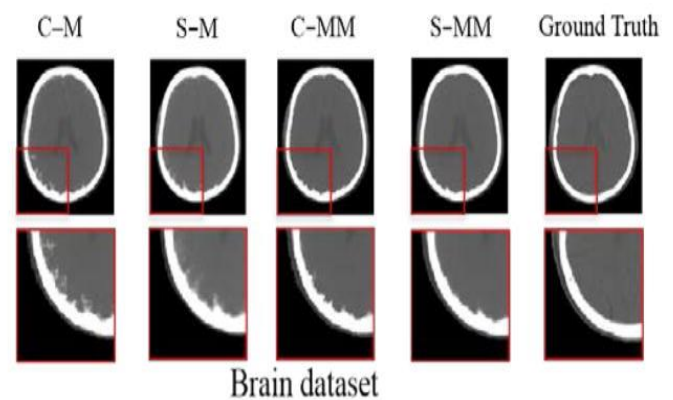


Figure 3: Considered Images from Dataset

Qualitative comparison of predictive results arising from ordinary adjustments inside the place of random wooden in databases: 1) upper panel and 2) decrease panel. All panels are, from left to right, dash line shows effects for predicting the usage of a random wooded region with a top-notch ensemble model (TN-M), a randomly advanced wooden with an propose ensemble model (MF-M), a wooded location median of functionality ensemble version (MF-MM). TN-MM, a randomly constructed wooded area with a mean of capability ensemble version (MF-MM), and an actual CT floor. The back row shows the closure of the areas proven inside the crimson rectangle in the purple line. Tables 1 further illustrate the above quantity. Since the effects from wonderful variations differ drastically in regions of easy tissue (mainly in regions of bone marrow, as regarded in Figure. 3), we grant results solely inner such a place. Tables 1 most probably reflect the standard spellings of a randomly built wood area in a normal wooded location (TN-M vs. MF-M, and TN-MM vs. MF-MM), as properly

because of the median ordinary performance of the capacity ensemble version in distinction to the preferred ability i version (TN-MM competes with TN-M, and MF-MM competes with MF-M). In addition to displaying the statistical magnitude of the development, we executed a random hypothesis on the usage of the acquired consequences. The following p values for every database are a good deal less than 0.05.

Table 1: Comparison of quantity relation of CT images, in accordance to MAE and PSNR on brain dataset

| MAE | Mean ± s.d | Med. | 15 th -portion | 65 th -portion |
|-------|------------|------|---------------------------|---------------------------|
| TN-M | 33.3±7.8 | 35.0 | 22.0 | 47.2 |
| MF-M | 34.5±9.0 | 36.7 | 17.8 | 43.3 |
| TN-MM | 22.5±4.5 | 24.6 | 18.9 | 34.9 |
| MF-MM | 23.4±4.3 | 24.6 | 16.0 | 32.0 |
| PSNR | Mean ± s.d | Med. | 15 th -portion | 65 th -portion |
| TN-M | 25.0 ± 2.1 | 26.7 | 22.9 | 25.8 |
| MF-M | 24.7 ± 1.1 | 27.6 | 23.5 | 26.7 |
| TN-MM | 26.6 ± 1.3 | 24.6 | 24.0 | 27.7 |
| MF-MM | 29.4 ± 1.2 | 28.9 | 26.6 | 28.4 |

4. Conclusion

In this paper predicted CT images were extracted from MRI images with PET attenuation correction approach. This approach helps in just not increasing the performance of prediction of CT images but also reduces the radiation exposure of the body. The performance metrics MAE and PSNR were varied by 18±5.6% and 23.65±5.54% respectively. Out of all existing schemes the proposed model was enhanced its results in terms of correlation by 0.3% increase.

References

- [1]. L. G. Strauss and P. S. Conti, "The applications of PET in clinical oncology," *J. Nucl. Med.* 32, 623–648.
- [2]. Nouby M. Ghazaly, M. M. A. . (2022). A Review on Engine Fault Diagnosis through Vibration Analysis . *International Journal on Recent Technologies in Mechanical and Electrical Engineering*, 9(2), 01–06. <https://doi.org/10.17762/ijrmee.v9i2.364>
- [3]. Brenner DJ, Hall EJ. Computed Tomography — An Increasing Source of Radiation Exposure. *New England Journal of Medicine*. 2007;357(22):2277–2284.
- [4]. Zaidi H, Montandon ML, Slosman DO. Magnetic resonance imaging-guided attenuation and scatter corrections in three-dimensional brain positron emission tomography. *Medical Physics*. 2003;30(5):937–948.

- [5]. Hsu S-H, et al. Investigation of a method for generating synthetic CT models from MRI scans of the head and neck for radiation therapy. *Physics in medicine and biology*. 2013;58(23) doi: 10.1088/0031-9155/58/23/8419.
- [6]. Berker Y, et al. MRI-Based Attenuation Correction for Hybrid PET/MRI Systems: A 4-Class Tissue Segmentation Technique Using a Combined Ultrashort-Echo-Time/Dixon MRI Sequence. *Journal of Nuclear Medicine*. 2012;53(5):796–804.
- [7]. Kops ER, Herzog H. Alternative methods for attenuation correction for PET images in MR-PET scanners. *Nuclear Science Symposium Conference Record, 2007. NSS '07. IEEE; 2007*.
- [8]. Yu Gong^{1,3}, Hongming Shan², Yueyang Teng^{*1}, Hairong Zheng ³, Ge Wang², Shanshan Wang^{*3}, LOW-DOSE PET IMAGE RESTORATION WITH 2D AND 3D NETWORK PRIOR LEARNING, 978-1-7281-7401-3/20/\$31.00 ©2020 IEEE
- [9]. Lijun Zhao, Zixiao Lu, Jun Jiang, Yujia Zhou, Yi Wu, and Qianjin Feng, "Automatic nasopharyngeal carcinoma segmentation using fully convolutional networks with auxiliary paths on dual-modality pet-ct images," *Journal of digital imaging*, vol. 32, no. 3, pp. 462–470, 2019.
- [10]. Andersen FL, Ladefoged CN, Beyer T, et al. Combined PET/MR imaging in neurology: MR-based attenuation correction implies a strong spatial bias when ignoring bone. *Neuroimage*. 2014;84: 206–216.
- [11]. Kadhim, R. R., and M. Y. Kamil. "Evaluation of Machine Learning Models for Breast Cancer Diagnosis Via Histogram of Oriented Gradients Method and Histopathology Images". *International Journal on Recent and Innovation Trends in Computing and Communication*, vol. 10, no. 4, Apr. 2022, pp. 36-42, doi:10.17762/ijritcc.v10i4.5532.
- [12]. Roy S, Carass A, Jog A, et al. MR to CT registration of brains using image synthesis. *Proc SPIE*. March 21, 2014:9034.
- [13]. Keller, S.H., Holm, S., Hansen, A.E., Sattler, B., Andersen, F., Klausen, T.L., Højgaard, L., Kjær, A., Beyer, T., 2013. Image artifacts from MR-based attenuation correction in clinical, whole-body PET/MRI. *MAGMA* 26 (1), 173–181.
- [14]. A. Jog, S. Roy, A. Carass, and J. L. Prince, "Magnetic Resonance Image Synthesis through Patch Regression," in *Proc. of the Int. Symposium on Biomed. Imag. (ISBI 2013)*, 2013, pp. 350–353.
- [15]. L. N. Balai, G. K. J. A. K. S. (2022). Investigations on PAPR and SER Performance Analysis of OFDMA and SCFDMA under Different Channels. *International Journal on Recent Technologies in Mechanical and Electrical Engineering*, 9(5), 28–35. <https://doi.org/10.17762/ijrmee.v9i5.371>
- [16]. Li R, et al. Deep Learning Based Imaging Data Completion for Improved Brain Disease Diagnosis. In: Golland P, et al., editors. *Medical Image Computing and Computer-Assisted Intervention – MICCAI 2014*. Springer International Publishing; 2014. pp. 305–312.
- [17]. Jung JH, Choi Y, Jung J, Kim S, Lim HK, Im KC, et al. Development of PET/MRI with insertable PET for

- simultaneous PET and MR imaging of human brain. *Med Phys.* 2015;42:2354– 63.
- [18]. Roy S, Carass A, Prince JL. Magnetic Resonance Image Example-Based Contrast Synthesis. *Medical Imaging, IEEE Transactions on.* 2013;32(12):2348–2363.
- [19]. C. Rorden, L. Bonilha, J. Fridriksson, B. Bender, and H. Karnath, “Agespecific CT and MRI templates for spatial normalization,” *NeuroImage*, vol. 61, no. 4, pp. 957–966, 2012.
- [20]. Ranadev, M. B. ., V. R. . Sheelavant, and R. L. . Chakrasali. “Predetermination of Performance Parameters of 3-Phase Induction Motor Using Numerical Technique Tools”. *International Journal on Recent and Innovation Trends in Computing and Communication*, vol. 10, no. 6, June 2022, pp. 63-69, doi:10.17762/ijritcc.v10i6.5628.
- [21]. Ye D, et al. Modality Propagation: Coherent Synthesis of Subject-Specific Scans with Data-Driven Regularization. In: Mori K, et al., editors. *Medical Image Computing and Computer-Assisted Intervention – MICCAI 2013*. Springer; Berlin Heidelberg: 2013. pp. 606–613.
- [22]. Kabisha, M. S., Rahim, K. A., Khaliluzzaman, M., & Khan, S. I. (2022). Face and Hand Gesture Recognition Based Person Identification System using Convolutional Neural Network. *International Journal of Intelligent Systems and Applications in Engineering*, 10(1), 105–115. <https://doi.org/10.18201/ijisae.2022.273>
- [23]. Cao, T., Zach, C., Modla, S., Powell, D., Czymmek, K., Niethammer, M.: Registration for Correlative Microscopy Using Image Analogies. In: Dawant, B.M., Christensen, G.E., Fitzpatrick, J.M., Rueckert, D. (eds.) *WBIR 2012*. LNCS, vol. 7359, pp. 296–306. Springer, Heidelberg (2012)
- [24]. Chaudhary, D. S. . (2022). Analysis of Concept of Big Data Process, Strategies, Adoption and Implementation. *International Journal on Future Revolution in Computer Science & Communication Engineering*, 8(1), 05–08. <https://doi.org/10.17762/ijfrcsce.v8i1.2065>